



# Design, synthesis and biological evaluation of novel *Pseudomonas aeruginosa* DNA gyrase B inhibitors

Sridhar Jogula<sup>a</sup>, Vagolu Siva Krishna<sup>a</sup>, Nikhila Meda<sup>a</sup>, Vadla Balraju<sup>b</sup>, Dharmarajan Sriram<sup>a,\*</sup>

<sup>a</sup> Department of Pharmacy, Birla Institute of Technology and Science-Pilani, Hyderabad Campus, Jawahar Nagar, Hyderabad 500078, India

<sup>b</sup> Albany Molecular Research Hyderabad Research Centre Private Limited, MN Park, Genome valley, Hyderabad 500078, India

## ARTICLE INFO

### Keywords:

*Pseudomonas aeruginosa*  
DNA gyrase B  
Molecular docking  
Molecular dynamics  
Isothiazole  
Oxazole

## ABSTRACT

In the present study, we attempted to develop a novel class of compounds active against *Pseudomonas aeruginosa* (Pa) by exploring the pharmaceutically well exploited enzyme targets. Since, lack of Pa gyrase B crystal structures, *Thermus thermophilus* gyrase B in complex with novobiocin (1KLJ) was used as template to generate model structure by performing homology modeling. Further the best model was validated and used for high-throughput virtual screening, docking and dynamics simulations using the *in-house* database for identification of Pa DNA gyrase B inhibitors. This study led to an identification of three lead molecules with IC<sub>50</sub> values in range of 6.25–15.6 μM against Pa gyrase supercoiling assay. **Lead-1** optimization and expansion resulted in 15 compounds. Among the synthesized compounds six compounds were shown good enzyme inhibition than **Lead-1** (IC<sub>50</sub> 6.25 μM). Compound **13** emerged as the most potential compound exhibiting inhibition of Pa gyrase supercoiling with an IC<sub>50</sub> of 2.2 μM; and in-vitro Pa activity with MIC of 8 μg/mL in presence of efflux pump inhibitor; hence could be further developed as novel inhibitor for Pa gyrase B.

## 1. Introduction

*Pseudomonas aeruginosa* (Pa) is a rod-shaped, gram-negative bacterium belonging to the family Pseudomonadacea and emerging worldwide as one of serious threats to human health [1]. A ubiquitous environmental and most common nosocomial isolates constituting of 20% in case of pediatric intensive care unit (PICU) [2] and 10% [3] of all hospital acquired infections. It is also termed as opportunistic human pathogen as it colonizes in immune compromised patients, like those with cystic fibrosis, cancer, or AIDS [4] rather than healthy individuals. Treatment against this pathogen remains challenging because of development of antibiotic resistance, an increasing threat to human health. It exhibits intrinsic resistance i.e. constitutive expression of AmpC b-lactamase and efflux pumps, combined with a low permeability of the outer membrane and its remarkable ability to acquire further resistance mechanisms to multiple groups of antimicrobial agents, including β-lactams, aminoglycosides and fluoroquinolones [5]. Hence, there is an immediate need in the identification and synthesis of novel drugs for potential targets that circumvents *Pseudomonas* infections.

A strategic approach to antimicrobial drug discovery is to target enzymes that are vital for the existence of the bacterium. In supports to this, DNA gyrase is an essential enzyme and has proven to be a worthy

target for antimicrobial agents. It belongs to a class of type II topoisomerase enzymes, a hetero-tetramer having two each subunits of A and B. An ATP dependent enzyme, controls topological transitions [6] by introducing negative super-coiling in double stranded closed circular DNA. Negative supercoiling maintains DNA in under winding state, helps in strand separation during replication.

The action of subunits A (GyrA) is inhibited by quinolones such as nalidixic acid and ciprofloxacin, while those of the B subunits (GyrB) are inhibited by coumarins such as coumermycin A<sub>1</sub> and novobiocin. Targeting gyrase may have an edge over others as it arrests DNA replication predominantly along with recombination, transcription and repair. While GyrA domain was exploited extensively, the GyrB catalytic domain has high scope for research. Pa has developed resistant towards fluoroquinolones and other available drugs. Most of the present drugs were specific to GyrA, but very few compounds were explored towards GyrB. Novobiocin is the only aminocoumarin till date that was approved against GyrB. The remarkable ability of Pa to acquire further resistance mechanism to multiple groups of available antimicrobial agents including β-lactams, aminoglycosides and fluoroquinolones provides a huge scope for finding structurally different compounds. Hence, the aim of present study is to identify new compounds acting specifically on GyrB subunit of *P. aeruginosa* [7].

\* Corresponding author.

E-mail address: [dsriram@hyderabad.bits-pilani.ac.in](mailto:dsriram@hyderabad.bits-pilani.ac.in) (D. Sriram).

## 2. Results and discussion

### 2.1. Homology modeling

*Pa* GyrB structure was generated by using the homology modeling by considering the *Thermus thermophilus* GyrB as a template [8]. Total of 20 structures were generated and 16th model with lowest discrete optimized potential energy (DOPE) score ( $-39058.39 \text{ kcal/mol}^{-1}$ ), was selected as the reliable one for further validation. It possess 98.5% residues in most favored regions of Ramachandran plot analysis which suggesting the model was good with decent stereo-chemical quality [9]. ProSA analysis resulted in z-score of  $-7.78$  revealed that the model is well within the range of native conformations of X-ray crystal structures and overall residue energies remain largely negative [10]. ProQ tool assessment showed LG score of 4.945 represents the model is of extremely good quality [11]. The model structure was visualized by using PyMOL [12].

### 2.2. Binding site analysis

The generated tertiary structure of drug target is the initial requirement for structure-based drug design. Incorporating ligands into the homology model from the structural template enhances overall accuracy of the predicted models which also helps in determining ligand binding pocket. The superposition of the overall atoms of the target-template reflects the close resemblance with experimental one and the interpreted lower RMSD of  $0.81 \text{ \AA}$  show higher structural conservation. The modeled structure in complex with novobiocin was explored to find residues such as Asn48, Asp51, Glu52, Asp75, Asp78, Gly79, Ile80, Pro81, Asp83, Ile96, Asn107, Lys112, Val120, Arg138, Thr167 present within the  $4 \text{ \AA}$  binding site region of novobiocin. Five hydrogen bonds were observed with residues Asn48, Asp75, Asp83, Lys105 and Arg138. The target-template sequence alignment showed that these residues were conserved and were used to generate grid for molecular docking studies (Fig. 1).

### 2.3. Virtual screening

A receptor grid of  $20 \text{ \AA} \times 20 \text{ \AA} \times 20 \text{ \AA}$  was generated around the novobiocin binding residues and *in-house* library molecules were allowed to dock within the grid by virtual screening workflow protocol [13]. Glide high throughput virtual screening identified 184 compounds and these were re-docked using standard precision (SP)

**Table 1**

Molecular interactions of the Lead compounds and novobiocin.

S. No	Name	XP G score (kcal/mol)	Interactions
1	Lead-1	-4.843	Asn48, Asp75, Gly79, Lys112, Thr167
2	Lead-2	-3.141	Asp51, Lys112
3	Lead-3	-4.682	Asn48, Lys112
4	Novobiocin	-3.119	Asn48, Asp75, Asn109, Arg138

docking, 18 compounds were observed to show significant glide score in SP docking hence re-docked using extra precision mode (XP) [14]. All compounds were evaluated for their activity using *Pa* DNA gyrase supercoiling assay and found that Lead-1, Lead-2 and Lead-3 were active with  $IC_{50}$  of  $6.2 \text{ \mu M}$ ,  $8.7 \text{ \mu M}$  and  $15.6 \text{ \mu M}$  respectively. Molecular interactions of the Lead and novobiocin were shown in Table 1 and Fig. 2.

Based on the Lead-1 molecular interactions and its biological potency, we have designed and synthesized 15 derivatives and also performed the molecular docking and dynamic simulations. Out of all synthesized derivatives, compound **13** [4-amino-N5-(2-((3-chloro-5-(trifluoromethyl) benzyl)amino)-2-oxoethyl)-N5-(2-methylbenzo[d]oxazol-6-yl)isothiazole-3,5-dicarboxamide] in complex with GyrB (Fig. 3) showed hydrogen bonds with binding site residues such as Asn48, Asp75, Gly79, Lys112, and Thr167. It also formed  $\pi$ - $\pi$  interaction with Phe106. Hydrogen bonds with Asn48 and Asp75 were retained by compound **13** when compared with both novobiocin and Lead-1 interactions. Residues, Gly79, Lys112, and Thr167 shown van der Waals interactions in case of novobiocin, the same residues were enhancing the binding affinity by forming the hydrogen bonds with compound **13**. The XP G score of compound **13** ( $-5.317$ ) shown to be better compared to novobiocin and Lead-1. Lead molecule and its derivatives have obeyed to Lipinski rule of 5 (Table 1 in supporting information) [15]. Thus, Lead-1 and compound **13** were proposed as potential *Pa* DNA GyrB inhibitors.

### 2.4. Chemistry

The designed molecules were synthesized by following synthetic approach that has been shown in Scheme 1, intermediate compounds like 2-methylbenzo[d]oxazol-6-amine (**III**), bezylamines **V(a-p)** [17] and 4-amino-3-carbamoylisothiazole-5-carboxylic acid (**X**) [16] are

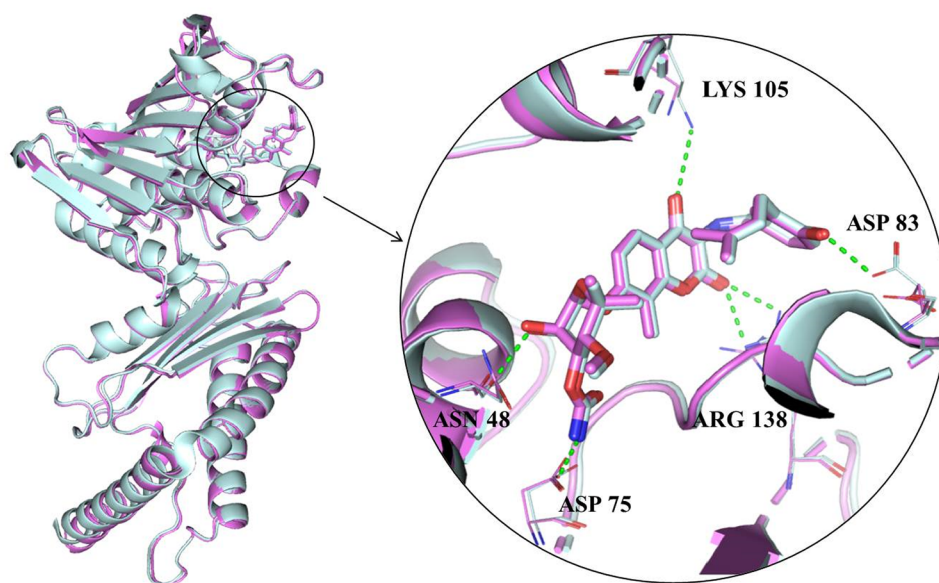


**Fig. 1.** Model structure of *Pseudomonas aeruginosa* GyrB, superimposed with template 1KIJ in the presence of novobiocin co-crystal ligand (RMSD =  $0.81 \text{ \AA}$ ). The color code representations for the picture are palegreen: template; violet: target. Conserved active site residues of target and template in the presence of novobiocin were labeled. The amino acids are represented in lines and novobiocin was in sticks.

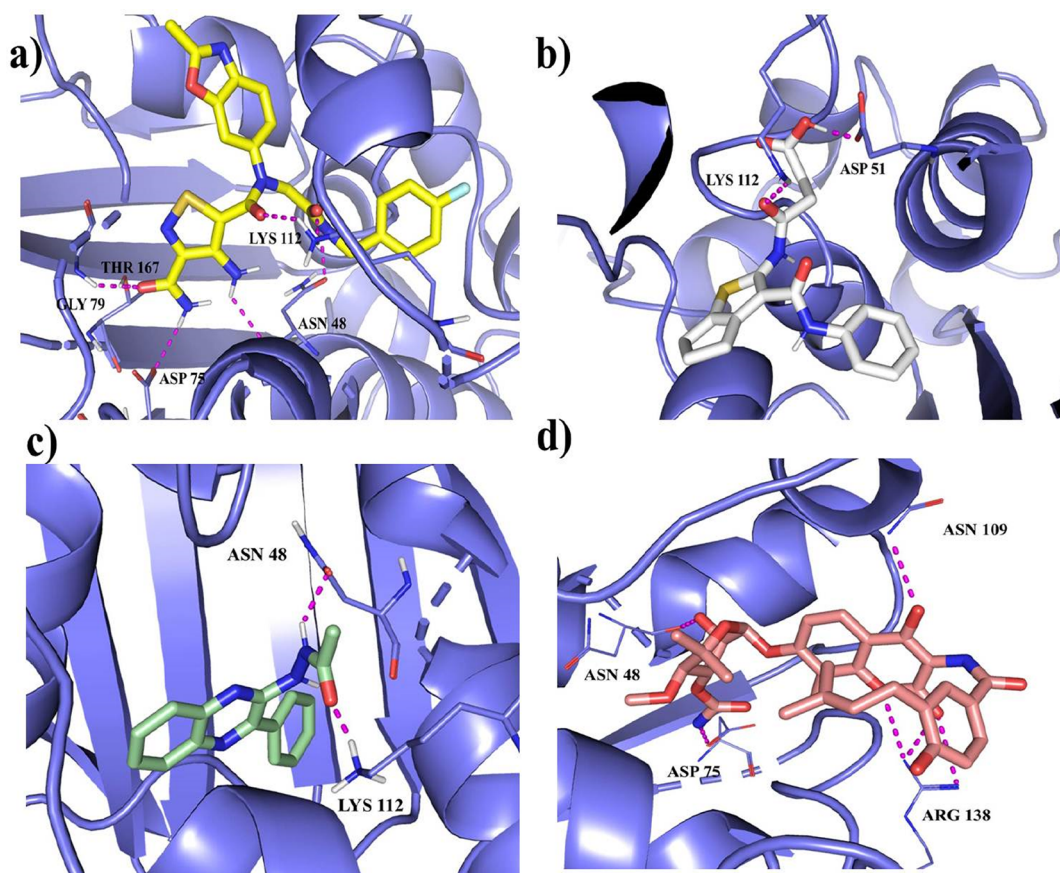


Fig. 2. Molecular docking of lead molecules and novobiocin with the *Pa* gyrase B homology model. a) Lead-1 (yellow) at active site of enzyme, b) Lead-2 (grey), c) Lead-3 (green), d) novobiocin (salmon red) docking confirmation at same active site and interactions with residues are in magenta color.

known and so followed literatures reported to synthesize them starting with commercially available and less expensive materials. 2-methylbenzo[d]oxazol-6-amine (III) prepared in two steps, in first step 2-Amino-5-nitrophenol (I) was treated with triethyl orthoacetate at reflux temperature as a neat reaction without any use of solvent gave 2-methyl-6-nitrobenzoxazole (II) in good yield. In step two, we used Zn/NH<sub>4</sub>Cl condition for reducing nitro to amine which gave very good conversion and also avoided handling Pd/H<sub>2</sub> chemistry, obtained 2-methylbenzo[d]oxazol-6-amine (III) with very good quality.

4-amino-3-carbamoylisothiazole-5-carboxylic acid (X) was prepared

in four steps [16], in first step; 2-cyanoacetamide (VI) as treated with sodium nitrite in presence of acetic acid and water to give compound VII, which upon reacting with 4-methylbenzenesulphonyl chloride gave compound VIII, which was cyclised using ethyl 2-mercaptoacetate to produce compound IX. Hydrolysis of compound IX gave 4-amino-3-carbamoylisothiazole-5-carboxylic acid (X).

Compounds V (a–p) were prepared by treating with 2-bromoacetyl bromide in presence of triethylamine with corresponding benzyl amines IV (a–p) [17]. Compound XI (a–p) were synthesized by *N*-alkylation of 2-methylbenzo[d]oxazol-6-amine (III) with corresponding

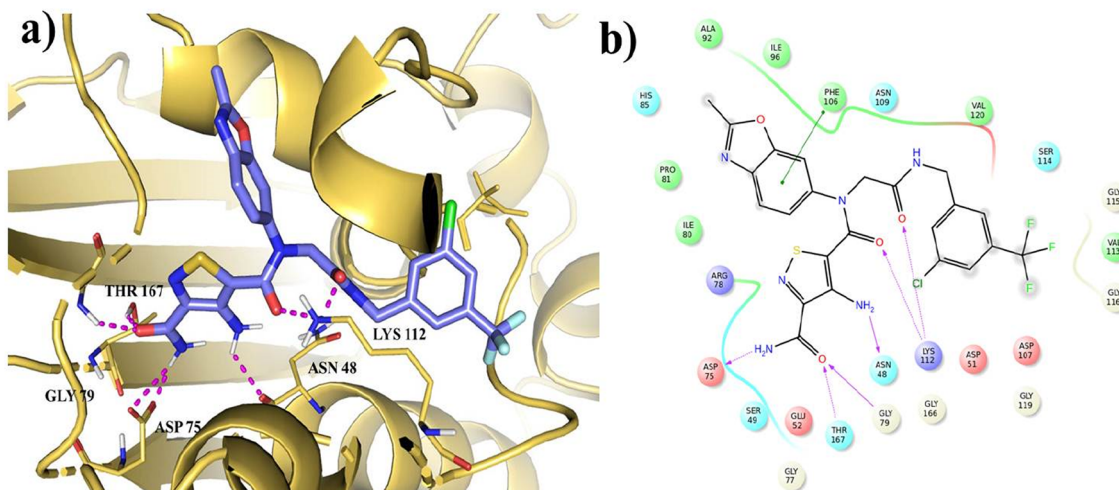
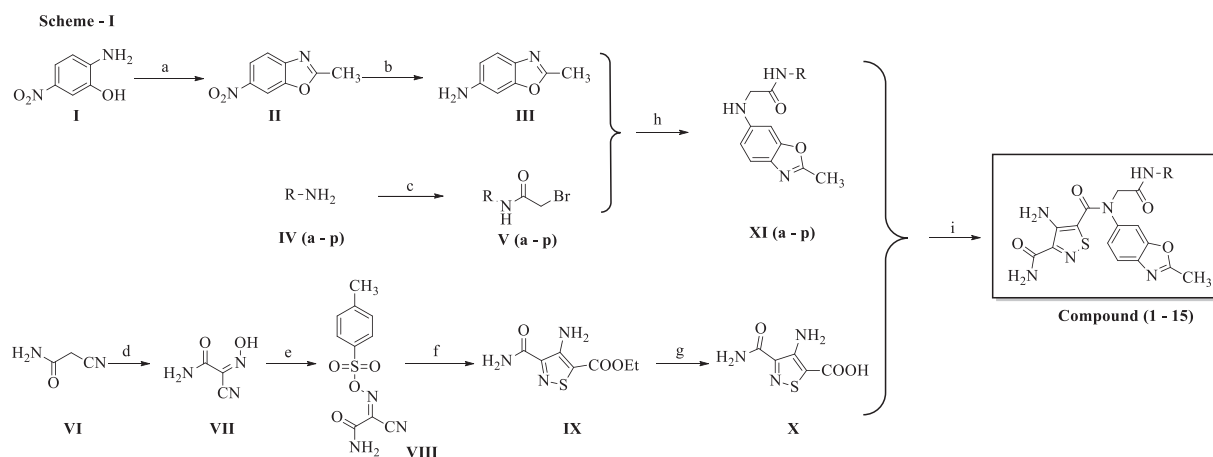
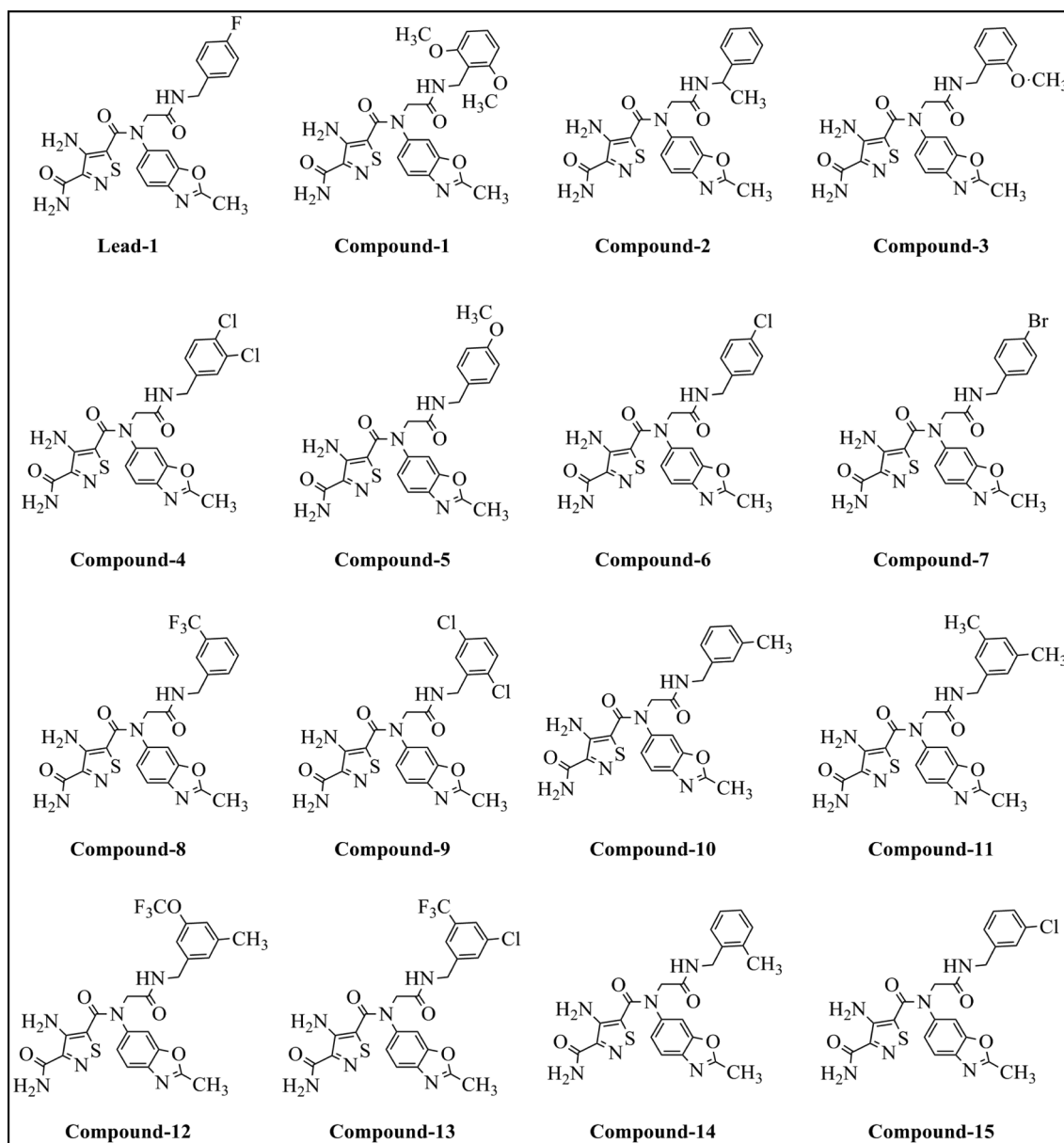


Fig. 3. Molecular interactions of compound 13 (blue color) shown in (a) 3D and (b) 2D representation.



**Scheme 1.** Synthetic protocol of the compounds, Reagents and conditions: (a) Triethyl orthoacetate, 110 °C, 12 h; (b) Zn, NH<sub>4</sub>Cl, THF:MeOH:H<sub>2</sub>O (1:1:1), 0–25 °C; (c) 2-bromoacetyl bromide, TEA, CH<sub>2</sub>Cl<sub>2</sub>, 0–25 °C, 2 h; (d) NaNO<sub>2</sub>, CH<sub>3</sub>COOH, H<sub>2</sub>O, 0–15 °C, 8 h; (e) 4-methylbenzenesulfonyl chloride, pyridine, 0–5 °C, 12 h; (f) ethyl 2-mercaptoacetate, piperidine, ethanol, 0–5 °C, 12 h; (g) NaOH, H<sub>2</sub>O, ethanol, rt, 12 h; (h) Cs<sub>2</sub>CO<sub>3</sub>, DMF, 80 °C, 3 h; (i) TBTU, triethylamine, ethylacetate, 3 h.



**Fig. 4.** Chemical structures of Lead-1 and compounds 1 to 15.

**Table 2**  
Synthesized compounds represented with substitutions along with their biological activities.

Compound	R	IC <sub>50</sub> μM	MIC <sup>a</sup> μg/mL	MIC <sup>b</sup> μg/mL	MIC <sup>c</sup> μg/mL
Lead-1	4-Fluorobenzyl	6.2 ± 0.9	> 64	–	–
1	2,6-Dimethoxybenzyl	> 10	> 64	–	–
2	1-Phenylethyl	> 10	64	–	–
3	2-Methoxybenzyl	10.0 ± 0.05	32	–	–
4	3,4-Dichlorobenzyl	4.5 ± 0.92	32	8	8
5	4-Methoxybenzyl	9.6 ± 0.81	64	–	–
6	4-Chlorobenzyl	6.6 ± 0.69	32	–	–
7	4-Bromobenzyl	4.2 ± 0.02	32	8	16
8	3-(Trifluoromethyl)benzyl	2.4 ± 0.99	64	–	–
9	2,5-Dichlorobenzyl	3.2 ± 0.53	> 64	16	16
10	3-Methylbenzyl	> 10	> 64	–	–
11	3,5-Dimethylbenzyl	> 10	> 64	–	–
12	3-Methyl-5-(trifluoromethoxy)benzyl	7.4 ± 0.56	> 64	–	–
13	3-Chloro-5-(trifluoromethyl)benzyl	2.2 ± 0.08	64	8	16
14	2-Methylbenzyl	> 10	> 64	–	–
15	3-Chlorobenzyl	5.2 ± 0.87	> 64	16	16

<sup>a</sup> Without efflux pump inhibitor.

<sup>b</sup> With phenylalanyl arginyl β-naphthylamide.

<sup>c</sup> With conessine.

compounds **V** (a – p) using cesium carbonate in DMF solvent. Final coupling reaction was also tried by using Boc protected compound **X** but failed to obtain desired product in good yield. Then the coupling reaction was performed using 4-amino-3-carbamoylisothiazole-5-carboxylic acid (**X**) and corresponding secondary amines **XI** (a – p) with 2-(1H-Benzotriazole-1-yl)-1,1,3,3-tetramethylammonium tetrafluoroborate (TBTU) and using ethylacetate as solvent to afford the Lead-1 and **1** to **15** compounds (Fig. 4).

## 2.5. Biological evaluation

All the synthesized compounds were screened for their *in-vitro* activity using *Pa* DNA gyrase supercoiling assay kit (Inspiralis, Norwich, UK) and results showed in (Table 2) [18,19]. Lead-1 possessing 4-fluorobenzyl group exhibited good *Pa* DNA GyrB inhibitory activity with an IC<sub>50</sub> value of 6.2 ± 0.9 μM. When, benzyl substitution of Lead-1 possessed electron withdrawing groups such as 4-chloro (IC<sub>50</sub>: 6.6 ± 0.69 μM), 4-bromo (IC<sub>50</sub>: 4.2 ± 0.02 μM) and 3-chloro (IC<sub>50</sub>: 5.2 ± 0.87 μM), the activity was not much deviated in comparison with Lead-1. When Lead-1 benzyl group possessed electron releasing groups such as 2,6-dimethoxy, 1-phenylethyl, 2-methoxy, 4-methoxy, 3-methyl, 3,5-dimethyl, 2-methyl, the activity was significantly reduced with IC<sub>50</sub> value of ≥ 10 μM. 3,4-dichlorobenzyl 3-(trifluoromethyl)benzyl, 2,5-dichlorobenzyl and 3-chloro-5-(trifluoromethyl)benzyl modifications on Lead-1 significantly enhanced the activity. **Compound 13** was found to be the most active with an IC<sub>50</sub> of 2.2 μM (Figs. 5a and 5b). Novobiocin was used as standard (positive control) and relaxed DNA without enzyme as blank (negative control). *In-vitro* activity of the synthesized molecules was evaluated against *P. aeruginosa* using broth dilution method [20]. Most of the compounds showed moderate activity as shown in Table 2. These molecules were not active (IC<sub>50</sub> value of > 10 μM) against DNA gyrase of *Staphylococcus aureus*, *Mycobacterium tuberculosis* and *Escherichia coli* indicates that it specifically active against *P. aeruginosa*.

The molecules were further tested *in-vitro* against *Pa* by agar dilution method. In the initial screening none of the compounds showed any appreciable activity (MIC of ≥ 32 μg/mL) even though showed good DNA gyrase inhibition. The inactivity might be due to the

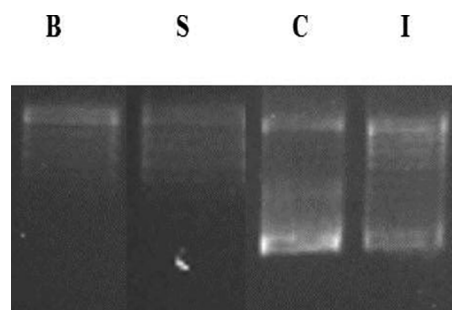


**Fig. 5a.** . Picture depicting the supercoiling assay of lead1. B - relaxed DNA; S - relaxed DNA + enzyme + Novobiocin (10 μM); C - relaxed DNA + enzyme; I - relaxed DNA + enzyme + lead1 (10 μM).

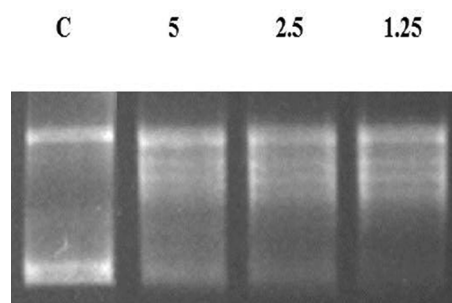


**Fig. 5b.** Picture depicting the supercoiling assay of active compound **13**. C - relaxed DNA + enzyme; compound **13** at different concentrations 5, 2.5, 1.25 (μM) + relaxed DNA + enzyme.

presence of efflux pump. Various chromosomally encoded efflux systems and outer membrane porins have been identified as important contributors to resistance in *Pa*. A number of MDR RND efflux pumps have been characterized in clinical isolates of *P. aeruginosa*, namely MexAB-OprM, MexCD-OprJ, MexEF-OprN, and MexXY-OprM. A number of potent efflux pump inhibitors including phenylalanyl arginyl β-naphthylamide (PAβN), carbonyl cyanide m-chloro-phenylhydrazone (CCCP), quinoline derivatives, conessine, and 1-(1-Naphthylmethyl)-piperazine (NMP) have been reported to enhance antibiotic activity against antibiotic-resistant Gram-negative bacteria. In view of this we further tested selected compounds in presence of PAβN and conessine and found that 2 to 8 times reduction in MIC (Table 2).

## 2.6. Molecular dynamics

Molecular dynamics simulations were carried out closer to the physiological environmental condition embedded with a system having water molecules, temperature and pressure [21,22]. The binding orientations of Lead-1 and compound **13** obtained after simulations showed better correlation with the biologically active states. Moreover, MD simulations quantify stability of the docked conformations. The dynamical properties of docking complex were analyzed from trajectories data obtained from 50 ns MD simulations through potential energy calculations, root mean square deviation (RMSD) and the stability of *P. aeruginosa* DNA GyrB with Lead-1 and compound **13** complexes was evaluated.

The root mean square deviation range for protein Cα and Lead-1 to their initial conformation was an average of 5.5 Å and 3.7 Å respectively, which was showed that after a small rearrangement from the initial conformation of complex up to first 10 ns time, was stable during entire MD simulations period (50 ns). Further the compound **13** has also shown the stability as Lead-1 with in the binding site. Compound **13** was more stable during the 50 ns with the average RMSD of 2.6 Å when compared with Lead-1. The RMSD plot analysis revealed that the

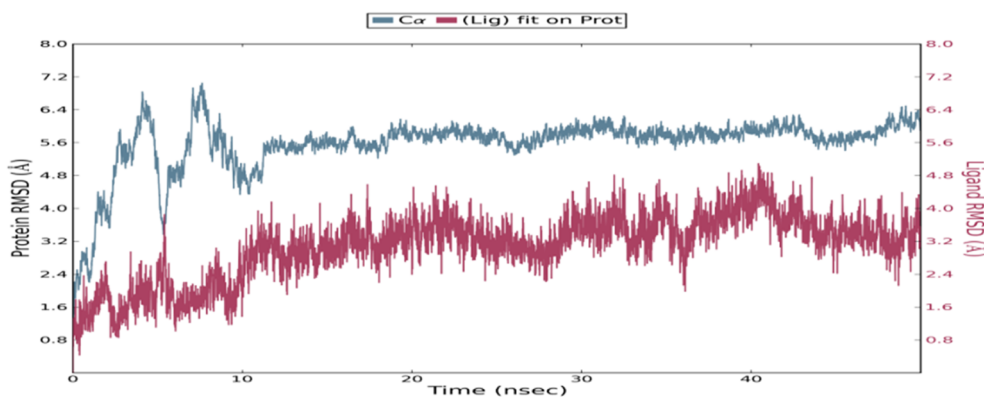


Fig. 6. Compound 13 RMSD plot with respect to time (50 ns).

*Pa* GyrB - compound 13 docking complex was stable in all 10,416 trajectories generated during 50 ns MD simulations time (Fig. 6).

### 3. Conclusion

In present work, molecular modeling, docking and dynamics simulations were employed to identify inhibitors of *Pseudomonas aeruginosa* DNA GyrB. Three molecules were found to be active with an  $IC_{50}$  below 15  $\mu$ M. Of these three, the best molecule was taken as Lead-1 and further optimized to synthesize fifteen novel compounds. These compounds were further evaluated by DNA gyrase supercoiling assay and observed six compounds were showing better  $IC_{50}$  values (2.2 – 6.25  $\mu$ M) compared to lead, compound 13 (4-amino-N5-(2-((3-chloro-5-(trifluoromethyl)benzyl)amino)-2-oxoethyl)-N5-(2-methylbenzo[d]oxazol-6-yl)isothiazole-3,5-dicarboxamide) being best with  $IC_{50}$  2.2  $\mu$ M. This was further supported by molecular docking and dynamics simulations showing that the compound 13 has better binding affinity and stability throughout 50 ns simulations time. Hence we believe that compound 13 would be an interesting lead for further optimization to synthesize novel *Pa* DNA GyrB inhibitor.

### 4. Experimental

#### 4.1. Homology modeling

Homology models are useful in structure-based drug designing applications, especially when a crystallographic structure is unavailable. Comparative structure modeling technique was implemented to predict the tertiary structure of *Pa* DNA gyrase using Modeller 9v13. *Pa* DNA gyrase B sequence (Q9I7C2) was retrieved from UniProt (<http://www.uniprot.org/>) and performed the BLAST search against PDB to identify the similar structural availability. Crystal structure of 43 K ATPase domain of *Thermus thermophilus* GyrB in complex with novobiocin was chosen as structural template (1KLJ) with structural identity of 46% through BLASTP against PDB analysis. CLUSTALX was used for initial target–template alignment. The alignment file was converted to Modeller input format (.ali) and modeler python script was defined to include heteroatoms during homology modeling. Twenty homology models were constructed based on satisfaction of target–template spatial restraints using Modeller9v13. The most reliable model was selected through DOPE score evaluations. The selected model was evaluated through RAMPAGE for assessment of Ramachandran plot, ProSA and ProQ. The validated *Pa* DNA gyrase model's novobiocin binding site was considered as target residues for the rational drug design and they were visualized using PyMOL.

#### 4.2. Protein preparation

The *Pa* DNA GyrB model was preprocessed with the protein

preparation workflow in the Maestro v9.6 (Schrodinger LLC, 2015). All hydrogens were added which were subsequently minimized with optimized potentials for liquid simulations (OPLS) 2005 force field and the impact molecular mechanics engine. Minimization was performed restraining the heavy atoms with the hydrogen torsion parameters turned off, to allow free rotation of the hydrogens setting the root mean square deviation (RMSD) of 0.3 Å. Active site residues were obtained from the template structure ligand interactions and a grid was generated around centroid of these residues.

#### 4.3. Virtual screening

Virtual screening is of key significance for the *in-silico* drug discovery process to accelerate drug development, as it helps in the selection of the best drug candidates. The prepared *in-house* database molecules were docked into the binding sites of the protein by using HTVS protocol for the assessment of protein–ligand binding affinities. The filtered molecules from HTVS were exposed to Glide SP (standard precision) docking which can dock tens to hundreds of ligands with high accuracy. Post-docking minimization was implemented to optimize the ligand geometries. Compounds with best docking and Glide scores were then subjected to Glide XP (extra precision) docking for further removal of false positives is achieved by extensive sampling and progressive scoring, resulting in advanced enrichment. High oral availability is often an important consideration for the development of bioactive molecules as therapeutic agents. Significant descriptors and pharmaceutically relevant properties (ADME properties) for the compounds were predicted for the development of a successful drug.

The *Pa* DNA GyrB modeled structure was optimized by adding hydrogen atoms and energy minimization to improve favorable steric contacts. A receptor grid of 20 Å x 20 Å x 20 Å was generated around novobiocin binding site and directed towards molecular docking for virtual screening from prepared ligand dataset of around 3000 compounds (*in-house* database). The binding affinity, interaction with surrounding residues, binding orientation of few compounds was observed to be better when compared to novobiocin. The Lead-1 ( $IC_{50}$  of 6.25  $\mu$ M) from the biological data has been taken for further optimization. The newly synthesized 15 analogues of Lead-1 were also performed the molecular docking and dynamics simulation studies to evaluate their mode of binding and stability in the binding pocket.

#### 4.4. Chemistry

Reagents obtained from commercial sources were used directly without further purification. Reactions were carried out under inert atmosphere of nitrogen or argon. All the reactions were monitored by thin layer chromatography (TLC) on silica gel 40 F254 (Merck, Darmstadt, Germany) coated on aluminium plates.  $^1$ H and  $^{13}$ C NMR spectra were recorded on a Bruker AM-400 NMR spectrometer, Bruker

BioSpin Corp., Germany. Chemical shifts are in parts per million (ppm) using tetramethylsilane as internal standard.

#### 4.4.1. Procedure for synthesis of 2-methyl-6-nitrobenzoxazole (II)

A mixture of Triethyl orthoacetate (80 mL) and 2-Amino-5-nitrophenol (I) (10.0 g) were refluxed for overnight under nitrogen, the reaction mixture was cooled 0 °C. Precipitated solids were filtered and obtained solids were charged with hexanes (100 mL), the slurry was stirred for 30 min. Filtered the solids and dried to afford 8.20 g of 2-methyl-6-nitrobenzoxazole (II) as pale yellow solid with the yield 76%. Analytical data for II: mp = 170–173 °C; <sup>1</sup>H NMR (400 MHz, CDCl<sub>3</sub>): δ 8.37 (d, *J* = 2.3 Hz, 1H), 8.26 (d, *J* = 2.3 Hz, 1H), 7.72 (d, *J* = 8.9 Hz, 1H), 2.71 (s, 3H); <sup>13</sup>C NMR (100 MHz, CDCl<sub>3</sub>): δ 168.7, 150.0, 146.8, 120.3, 119.3, 106.8, 100.5, 14.8. MS (ESI) Calc. for [C<sub>8</sub>H<sub>6</sub>N<sub>2</sub>O<sub>3</sub> + H]<sup>+</sup> = 179.14, found 179.09.

#### 4.4.2. Procedure for synthesis of 2-methylbenzo[d]oxazol-6-amine (III)

To a solution of 2-methyl-6-nitrobenzoxazole II (2.20 g, 12.36 mmol) in THF:MeOH:H<sub>2</sub>O (1:1:1, 30 mL) was charged NH<sub>4</sub>Cl (123.6 mmol). Reaction mixture cooled to 0–5 °C, charged zinc powder (123.6 mmol) portion wise, after the addition reaction mixture stirred at 10–15 °C for 2 h (monitored by TLC). Reaction mixture filtered through celite bed, filtrate charged with water (30 mL) and extracted with EtOAc (2 × 30 mL). The combined organic layer was washed with brine (20 mL), dried over anhydrous Na<sub>2</sub>SO<sub>4</sub>, filtered and evaporated under reduced pressure to afford 2-methylbenzo[d]oxazol-6-amine III as light brown solid with yield 78%. Analytical data for III: mp = 146–147 °C; <sup>1</sup>H NMR (400 MHz, DMSO-*d*<sub>6</sub>): δ 7.27 (d, *J* = 8.40 Hz, 1H), 6.74 (s, 1H), 6.56 (d, *J* = 6.4 Hz, 1H), 5.25 (s, 2H), 2.48 (s, 3H); <sup>13</sup>C NMR (100 MHz, DMSO-*d*<sub>6</sub>): δ 160.01, 151.83, 146.91, 131.38, 118.73, 111.53, 94.43, 13.85. MS (ESI) Calc. for [C<sub>8</sub>H<sub>8</sub>N<sub>2</sub>O + H]<sup>+</sup> = 148.16, found 148.08.

#### 4.4.3. General procedure for preparation of compounds Va – Vp

Substituted Benzyl amine IV (a–p) (10 mmol) in dichloromethane (50 mL) charged with triethylamine (12 mmol), and cooled to 0 °C. 2-bromoacetyl bromide (11 mmol) was added drop wise, continued stirring for 2 h at room temperature (monitored by TLC). The resulting mixture was concentrated under reduced pressure and the residue was purified by column chromatography using EtOAc/Hexanes as eluent to afford the desired product Va – Vp.

#### Analytical data of compounds Va – Vp:

##### 4.4.4. 2-Bromo-N-(4-fluorobenzyl)acetamide (Va)

Yield: 82%; brown solid; mp = 163–165 °C; MS(ESI): <sup>1</sup>H NMR (400 MHz, CDCl<sub>3</sub>): δ 8.83 (s, 1H), 7.25 (d, *J* = 7.82 Hz, 2H), 7.04 (d, *J* = 8.82 Hz, 2H), 4.45 (d, *J* = 5.7 Hz, 2H), 3.96 (s, 2H). <sup>13</sup>C NMR (100 MHz, CDCl<sub>3</sub>): δ 170.84, 162.4, 133.2, 129.5, 115.73, 43.1, 28.4. MS (ESI) Calc. for [C<sub>9</sub>H<sub>9</sub>BrNO + H]<sup>+</sup> = 246.99, found 246.98.

##### 4.4.5. 2-Bromo-N-(2,6-dimethoxybenzyl)acetamide (Vb)

Yield: 79%; white solid; mp = 181–183 °C; <sup>1</sup>H NMR (400 MHz, CDCl<sub>3</sub>): δ 7.14 (d, *J* = 8.83 Hz, 1H), 7.08 (d, *J* = 8.83 Hz, 2H), 6.27 (bs, 1H), 4.51 (d, *J* = 5.7 Hz, 2H), 3.89 (s, 2H), 2.37 (s, 6H). <sup>13</sup>C NMR (100 MHz, CDCl<sub>3</sub>): δ 170.8, 156.7, 128.2, 115.1, 104.7, 57.3, 30.8, 28.4. MS (ESI) Calc. for [C<sub>11</sub>H<sub>14</sub>BrNO<sub>3</sub> + H]<sup>+</sup> = 289.01, found 248.02.

##### 4.4.6. 2-Bromo-N-(1-phenylethyl)acetamide (Vc)

Yield: 76%; brown solid; mp = 221–223 °C; <sup>1</sup>H NMR (400 MHz, CDCl<sub>3</sub>): δ 7.41–7.21 (m, 5H), 6.70 (s, 1H), 5.19–5.05 (m, 1H), 3.87 (d, *J* = 6.6 Hz, 2H), 1.55 (s, 3H). <sup>13</sup>C NMR (100 MHz, CDCl<sub>3</sub>): δ 171, 134.3, 128.9, 127.1, 126.8, 53.2, 30.3, 28.4. MS (ESI) Calc. for [C<sub>11</sub>H<sub>12</sub>BrNO + H]<sup>+</sup> = 243.01, found 243.06.

##### 4.4.7. 2-Bromo-N-(2-methoxybenzyl)acetamide (Vd)

Yield: 65%; white solid; mp = 197–199 °C; <sup>1</sup>H NMR (400 MHz,

CDCl<sub>3</sub>): δ 8.59 (s, 1H), 7.27–7.23 (t, *J* = 8.0 Hz, 1H), 7.18 (d, *J* = 7.2 Hz, 1H), 6.99 (d, *J* = 8.4 Hz, 1H), 6.93–6.89 (t, *J* = 7.2 Hz, 1H), 4.25 (d, *J* = 5.6 Hz, 2H), 3.92 (s, 2H), 3.80 (s, 3H). <sup>13</sup>C NMR (100 MHz, CDCl<sub>3</sub>): δ 173.4, 156.3, 128.3, 128.1, 127.4, 122.3, 113.6, 55.8, 35.7, 28.6. MS (ESI) Calc. for [C<sub>10</sub>H<sub>12</sub>BrNO<sub>2</sub> + H]<sup>+</sup> = 259.00, found 249.00.

##### 4.4.8. 2-Bromo-N-(3,4-dichlorobenzyl)acetamide (Ve)

Yield: 82%; yellow solid; mp = 206–208 °C; <sup>1</sup>H NMR (400 MHz, CDCl<sub>3</sub>): δ 8.86 (s, 1H), 7.61 (d, *J* = 8.0 Hz, 1H), 7.52 (s, 1H), 7.27 (d, *J* = 8.40 Hz, 1H), 4.30 (d, *J* = 6.0 Hz, 2H), 3.92 (s, 2H). <sup>13</sup>C NMR (100 MHz, CDCl<sub>3</sub>): δ 173.2, 144.7, 131.5, 130.2, 129.8, 128.3, 127.6, 42.4, 28.9. MS (ESI) Calc. for [C<sub>9</sub>H<sub>8</sub>BrCl<sub>2</sub>NO + H]<sup>+</sup> = 298.91, found 298.90.

##### 4.4.9. 2-Bromo-N-(4-methoxybenzyl)acetamide (Vf)

Yield: 89%; brown solid; mp = 187–189 °C; <sup>1</sup>H NMR (400 MHz, CDCl<sub>3</sub>): δ 8.70 (s, *J* = 8.8 Hz, 1H), 7.19 (d, *J* = 8.40 Hz, 2H), 6.89 (d, *J* = 8.40 Hz, 2H), 4.22 (d, *J* = 5.6 Hz, 2H), 3.88 (s, 2H), 3.72 (s, 3H). <sup>13</sup>C NMR (100 MHz, CDCl<sub>3</sub>): δ 173.2, 156.6, 131.3, 130.8, 115.1, 55.2, 43.6, 28.9. MS (ESI) Calc. for [C<sub>10</sub>H<sub>12</sub>BrNO<sub>2</sub> + H]<sup>+</sup> = 259.00, found 259.10.

##### 4.4.10. 2-Bromo-N-(4-chlorobenzyl)acetamide (Vg)

Yield: 74%; pale yellow solid; mp = 203–205 °C; <sup>1</sup>H NMR (400 MHz, CDCl<sub>3</sub>): δ 8.82 (s, 1H), 7.40 (d, *J* = 8.40 Hz, 2H), 7.29 (d, *J* = 8.40 Hz, 2H), 4.28 (d, *J* = 5.6 Hz, 2H), 3.91 (s, 2H). <sup>13</sup>C NMR (100 MHz, CDCl<sub>3</sub>): δ 172.9, 136.8, 133.7, 131.8, 127.8, 43.1, 28.4. MS (ESI) Calc. for [C<sub>9</sub>H<sub>9</sub>BrClNO + H]<sup>+</sup> = 262.95, found 263.09.

##### 4.4.11. 2-Bromo-N-(4-bromobenzyl)acetamide (Vh)

Yield: 81%; brown solid; mp = 235–237 °C; <sup>1</sup>H NMR (400 MHz, CDCl<sub>3</sub>): δ 8.73 (s, 1H), 7.51 (d, *J* = 8.83 Hz, 2H), 7.22 (d, *J* = 8.83 Hz, 2H), 4.28 (d, *J* = 5.7 Hz, 2H), 3.86 (s, 2H). <sup>13</sup>C NMR (100 MHz, CDCl<sub>3</sub>): δ 172.9, 136.8, 131.9, 130.1, 122.8, 42.8, 28.8. MS (ESI) Calc. for [C<sub>9</sub>H<sub>9</sub>Br<sub>2</sub>NO + H]<sup>+</sup> = 306.90, found 307.00.

##### 4.4.12. 2-Bromo-N-(3-(trifluoromethyl)benzyl)acetamide (Vi)

Yield: 72%; yellow solid; mp = 251–253 °C; <sup>1</sup>H NMR (400 MHz, CDCl<sub>3</sub>): δ 8.87 (s, 1H), 7.51 (s, *J* = 8.84 Hz, 1H), 7.46 (t, *J* = 6.2 Hz, 1H), 7.41 (d, *J* = 8.82 Hz, 1H), 7.34 (d, *J* = 8.82 Hz, 1H), 4.29 (d, *J* = 5.7 Hz, 2H), 3.92 (s, 2H). <sup>13</sup>C NMR (100 MHz, CDCl<sub>3</sub>): δ 173.7, 138.4, 130.9, 130.6, 127.8, 124.6, 123.5, 123.1, 42.7, 28.9. MS (ESI) Calc. for [C<sub>10</sub>H<sub>9</sub>BrF<sub>3</sub>NO + H]<sup>+</sup> = 296.98, found 297.04.

##### 4.4.13. 2-Bromo-N-(2,5-dichlorobenzyl)acetamide (Vj)

Yield: 70%; brown solid; mp = 179–181 °C; <sup>1</sup>H NMR (400 MHz, CDCl<sub>3</sub>): δ 8.83 (s, 1H), 7.52 (d, *J* = 8.21 Hz, 1H), 7.46 (s, 1H), 7.39 (d, *J* = 8.19 Hz, 1H), 4.32 (d, *J* = 5.7 Hz, 2H), 3.90 (s, 2H). <sup>13</sup>C NMR (100 MHz, CDCl<sub>3</sub>): δ 174.7, 145.2, 132.2, 130.6, 130.2, 128.9, 128.5, 39.4, 28.8. MS (ESI) Calc. for [C<sub>9</sub>H<sub>8</sub>BrCl<sub>2</sub>NO + H]<sup>+</sup> = 296.91, found 297.02.

##### 4.4.14. 2-Bromo-N-(3-methylbenzyl)acetamide (Vk)

Yield: 70%; pale yellow solid; mp = 162–164 °C; <sup>1</sup>H NMR (400 MHz, CDCl<sub>3</sub>): δ 8.79 (s, 1H), 7.32 (t, *J* = 6.1 Hz, 1H), 7.11 (s, 1H), 7.06 (d, *J* = 7.78 Hz, 1H), 7.03 (d, *J* = 7.8 Hz, 1H), 4.26 (d, *J* = 5.8 Hz, 2H), 3.86 (s, 2H), 2.29 (s, 3H). <sup>13</sup>C NMR (100 MHz, CDCl<sub>3</sub>): δ 172.9, 138.2, 136.8, 129.1, 128.9, 127.4, 125.8, 45.1, 28.8, 22.1. MS (ESI) Calc. for [C<sub>10</sub>H<sub>12</sub>BrNO + H]<sup>+</sup> = 243.01, found 243.00.

##### 4.4.15. 2-Bromo-N-(3,5-dimethylbenzyl)acetamide (Vl)

Yield: 76%; white solid; mp = 175–177 °C; <sup>1</sup>H NMR (400 MHz, CDCl<sub>3</sub>): δ 8.77 (s, 1H), 7.21 (s, 1H), 7.16 (s, 1H), 7.12 (s, 1H), 4.25 (d, *J* = 5.6 Hz, 2H), 3.84 (s, 2H), 2.27 (s, 6H). <sup>13</sup>C NMR (100 MHz, CDCl<sub>3</sub>): δ 172.1, 142.1, 137.9, 128.6, 125.9, 44.2, 28.7, 21.6. MS (ESI) Calc. for

$[C_{11}H_{14}BrNO + H]^+ = 257.02$ , found 257.08.

#### 4.4.16. 2-Bromo-N-(3-methyl-5-(trifluoromethoxy)benzyl)acetamide (Vm)

Yield: 78%; brown solid; mp = 241–243 °C;  $^1H$  NMR (400 MHz,  $CDCl_3$ ):  $\delta$  8.79 (s, 1H), 7.13 (s, 1H), 7.09 (s, 1H), 7.07 (s, 1H), 4.24 (d,  $J = 5.8$  Hz, 2H), 3.82 (s, 2H), 2.31 (s, 3H).  $^{13}C$  NMR (100 MHz,  $CDCl_3$ ):  $\delta$  175.2, 161.4, 143.2, 142.5, 130.1, 123.9, 113.5, 109.1, 43.3, 28.8, 21.8. MS (ESI) Calc. for  $[C_{11}H_{11}BrF_3NO_2 + H]^+ = 326.99$ , found 327.01.

#### 4.4.17. 2-Bromo-N-(3-chloro-5-(trifluoromethyl)benzyl)acetamide (Vn)

Yield: 78%; white solid; mp = 206–208 °C;  $^1H$  NMR (400 MHz,  $CDCl_3$ ):  $\delta$  8.88 (s, 1H), 7.69 (s, 1H), 7.47 (s, 1H), 7.42 (s, 1H), 4.29 (d,  $J = 5.8$  Hz, 2H), 3.92 (s, 2H).  $^{13}C$  NMR (100 MHz,  $CDCl_3$ ):  $\delta$  175.7, 145.1, 133.7, 132.4, 131.8, 123.5, 122.8, 120.9, 43.3, 28.8. MS (ESI) Calc. for  $[C_{10}H_8BrClF_3NO + H]^+ = 330.94$ , found 331.02.

#### 4.4.18. 2-Bromo-N-(2-methylbenzyl) acetamide (Vo)

Yield: 83%; brown solid; mp = 161–163 °C;  $^1H$  NMR (400 MHz,  $CDCl_3$ ):  $\delta$  8.79 (s, 1H), 7.38 (t,  $J = 6.62$  Hz, 1H), 7.36 (d,  $J = 7.7$  Hz, 1H), 7.28 (d,  $J = 7.7$  Hz, 1H), 7.22 (m, 1H), 4.24 (d,  $J = 5.6$  Hz, 2H), 3.82 (s, 2H), 2.34 (s, 3H).  $^{13}C$  NMR (100 MHz,  $CDCl_3$ ):  $\delta$  171.6, 141.4, 134.2, 130.6, 126.3, 125.6, 125.1, 41.8, 28.2, 18.2. MS (ESI) Calc. for  $[C_{10}H_{12}BrNO + H]^+ = 243.01$ , found 243.00.

#### 4.4.19. 2-Bromo-N-(3-chlorobenzyl)acetamide (Vp)

Yield: 74%; mp = 176–178 °C; white solid;  $^1H$  NMR (400 MHz,  $CDCl_3$ ):  $\delta$  8.82 (s, 1H), 7.46 (s, 1H), 7.37 (m, 2H), 7.21 (d,  $J = 8.2$  Hz, 1H), 4.28 (d,  $J = 5.8$  Hz, 2H), 3.89 (s, 2H).  $^{13}C$  NMR (100 MHz,  $CDCl_3$ ):  $\delta$  173.3, 144.1, 134.1, 130.6, 130.6, 127.8, 127.2, 42.3, 28.2. MS (ESI) Calc. for  $[C_9H_9BrClNO + H]^+ = 262.95$ , found 263.09.

#### 4.4.20. Procedure for synthesis of 2-amino-N-hydroxy-2-oxoacetimidoyl cyanide (VII)

A solution of 2-cyanoacetamide (VI) (1 mol) in AcOH (200 mL) was cooled to 0 °C and charged drop wise an aqueous solution of pre-dissolved sodium nitrite (2.5 mol). The reaction mixture was stirred at 15 °C for 8 h. The resulting solids were filtered, dried under reduced pressure to furnish 2-amino-N-hydroxy-2-oxoacetimidoyl cyanide (VII) with 70% yield and the crude material was used as such in next step without any further purification.

#### 4.4.21. Procedure for synthesis of 2-amino-2-oxo-N-(tosyloxy)acetimidoyl cyanide (VIII)

To a solution of 2-amino-N-hydroxy-2-oxoacetimidoyl cyanide (VII) (0.25 mol) in anhydrous pyridine (100 mL) was added 4-methylbenzenesulphonyl chloride (0.27 mol) drop wise at 0–5 °C, slowly allowed to warm to room temperature and stirred for 12 h. After completion of the reaction by TLC analysis, it was charged with ethanol (300 mL) and resulting solid was filtered, washed with cold ethanol and dried under reduced to afford 2-amino-2-oxo-N-(tosyloxy)acetimidoyl cyanide (VIII) with 75% yield. Thus obtained crude material was used as such in next step without any further purification.

#### 4.4.22. Procedure for synthesis of ethyl 4-amino-3-carbamoylisothiazole-5-carboxylate (IX)

A solution of 2-amino-2-oxo-N-(tosyloxy)acetimidoyl cyanide (VIII) (0.2 mol) and ethyl 2-mercaptoacetate (0.21 mol) in ethanol (250 mL) was charged Piperidine (0.1 mol) at 0–5 °C. The reaction mixture was slowly warmed to room temperature and stirred for 12 h. After completion of the reaction by TLC analysis, it was cooled to –10 °C, the resulting precipitate formed was filtered, washed with cold ethanol (100 mL) and dried under reduced pressure to afford ethyl 4-amino-3-carbamoylisothiazole-5-carboxylate (IX) with 50% yield which was used as such in next step without any further purification.

#### 4.4.23. Procedure for synthesis of 4-amino-3-carbamoylisothiazole-5-carboxylic acid (X)

To a solution of ethyl 4-amino-3-carbamoylisothiazol-5-carboxylate (0.1 mol) in ethanol (100 mL) was added an aqueous solution (60 mL) of NaOH (0.2 mol) at room temperature and allowed to stir for overnight. After completion of the reaction by TLC analysis, the solvent was evaporated under reduced pressure to afford crude residue. The crude material was dissolved in water and the aqueous layer was washed with ethyl acetate (100 mL). Then, the aqueous layer acidified to pH 4 using concentrated HCl and resulting precipitated solid was filtered and dried under reduced pressure to afford 4-amino-3-carbamoylisothiazole-5-carboxylic acid (X) as white solid with 80% yield.

**Analytical data of compound X:** mp = 251–253 °C,  $^1H$  NMR (400 MHz, DMSO- $d_6$ ):  $\delta$  8.11 (s, 2H), 7.76 (s, 2H);  $^{13}C$  NMR (100 MHz, DMSO- $d_6$ ):  $\delta$  163.69, 162.71, 149.17, 148.87, 122.63. MS (ESI) Calc. for  $[C_5H_5N_3O_3S + H]^+ = 188.01$ , found 188.00.

#### 4.4.24. General procedure for preparation of compounds XI (a–p)

To a solution of compound 3 (3.37 mmol) in DMF (10 mL), charged respective compound V (a–p) (4.04 mmol) and heated to 80 °C. After 3 h, TLC analysis showed complete conversion of starting materials. The reaction mixture was cooled to room temperature, charged water (30 mL) and extracted with EtOAc (2 × 20 mL). The combined organic layer was washed with water (20 mL) followed by brine and concentrated under reduced pressure to obtain gummy liquid. This crude material was triturated with MTBE to afford desired product as solid and which used as such in next step without any further purification.

#### 4.4.25. General procedure for preparation of Lead-1 and compounds (1–15)

To a solution of compound 4-amino-3-carbamoylisothiazole-5-carboxylic acid X (100 mg, 0.534 mmol) and triethylamine (0.15 mL, 1.068 mmol) in EtOAc (8 mL) was added 2-(1H-Benzotriazole-1-yl) 1,2,3,3-tetramethyluronium tetrafluoroborate (TBTU: 1 equiv) and the mixture was stirred at room temperature for 10 min. Then corresponding amine 11 (a–p) (2 equiv) was added and the reaction was stirred at room temperature for 3 h (monitored by TLC). The mixture was washed with water and extracted with EtOAc. The organic layer was separated, dried over anhydrous  $Na_2SO_4$ , filtered and concentrated under reduced pressure to afford crude material. The crude was purified by column chromatography (silica gel 100–200 mesh) using EtOAc: Heptane (2:1) as eluent to afford compounds (1–15) respectively.

#### Analytical data of compounds Lead-1 and compounds (1–15):

#### 4.4.26. 4-Amino-N5-(2-((4-fluorobenzyl)amino)-2-oxoethyl)-N5-(2-methylbenzo[d]oxazol-6-yl)isothiazole-3,5-dicarboxamide (Lead-1)

Yield: 56%; off white solid; mp = 273–275 °C;  $^1H$  NMR (400 MHz, DMSO- $d_6$ ):  $\delta$  8.62 (t,  $J = 5.8$  Hz, 1H), 7.93 (d,  $J = 2.0$  Hz, 1H), 7.84–7.78 (m, 2H), 7.62–7.54 (m, 2H), 7.29–7.25 (m, 2H), 7.17–7.09 (m, 4H), 4.42 (s, 2H), 4.29 (d,  $J = 6.0$  Hz, 2H), 2.66 (s, 3H);  $^{13}C$  NMR (100 MHz, DMSO- $d_6$ ):  $\delta$  167.72, 166.31, 163.75, 162.42, 151.21, 150.41, 146.70, 142.18, 136.98, 135.37, 129.15, 129.07, 126.97, 122.11, 119.87, 115.0, 114.79, 113.20, 53.10, 41.42, 14.24. MS (ESI) Calc. for  $[C_{22}H_{19}FN_6O_4S + H]^+ = 483.12$ , found 483.31. HPLC showed 96.1% of purity.

#### 4.4.27. 4-Amino-N5-(2-((2,6-dimethoxybenzyl)amino)-2-oxoethyl)-N5-(2-ethylbenzo[d]oxazol-6-yl)isothiazole-3,5-dicarboxamide (1)

Yield 42%; brown solid; mp = 269–271 °C;  $^1H$  NMR (400 MHz, DMSO- $d_6$ ):  $\delta$  8.61 (t,  $J = 5.8$  Hz, 1H), 7.93 (d,  $J = 2.0$  Hz, 1H), 7.82–7.76 (m, 2H), 7.64–7.56 (m, 2H), 7.19–7.13 (m, 1H), 7.11–7.04 (m, 4H), 4.38 (d,  $J = 6.0$  Hz, 2H), 3.74 (s, 2H), 2.56 (s, 3H), 2.41 (s, 6H);  $^{13}C$  NMR (100 MHz, DMSO- $d_6$ ):  $\delta$  167.72, 166.31, 163.75, 162.42, 159.6, 151.21, 150.41, 146.70, 142.18, 136.98, 135.37, 126.82, 126.97, 122.11, 119.87, 115.0, 114.79, 113.20, 53.47, 52.71, 41.88, 14.27. MS (ESI) Calc. for  $[C_{24}H_{24}N_6O_6S + H]^+ = 525.15$ , found

525.28. HPLC showed 97.5% of purity.

**4.4.28. 4-Amino-N5-(2-methylbenzo[d]oxazol-6-yl)-N5-(2-oxo-2-((1-phenylethyl)amino)ethyl)isothiazole-3,5-dicarboxamide (2)**

Yield 32%; pale yellow solid; mp = 268–270 °C; <sup>1</sup>H NMR (400 MHz, DMSO-*d*<sub>6</sub>): δ 8.64 (t, *J* = 5.8 Hz, 1H), 7.85 (d, *J* = 2.0 Hz, 1H), 7.81–7.75 (m, 2H), 7.62–7.56 (m, 2H), 7.51–7.22 (m, 5H), 7.17 (s, 2H), 5.19–5.08 (m, 1H), 4.39 (s, *J* = 6.0 Hz, 2H), 2.55 (s, 3H), 1.59 (d, 3H); <sup>13</sup>C NMR (100 MHz, DMSO-*d*<sub>6</sub>): δ 164.89, 162.21, 161.72, 159.82, 151.29, 150.47, 144.70, 139.18, 136.58, 135.31, 129.25, 129.13, 126.02, 125.87, 122.11, 119.87, 115.0, 114.79, 113.20, 53.47, 49.63, 24.68, 14.24. MS (ESI) Calc. for [C<sub>23</sub>H<sub>22</sub>N<sub>6</sub>O<sub>4</sub>S + H]<sup>+</sup> = 478.14, found 479.15. HPLC showed 95.4% of purity.

**4.4.29. 4-Amino-N5-(2-((2-methoxybenzyl)amino)-2-oxoethyl)-N5-(2-methylbenzo[d]oxazol-6-yl)isothiazole-3,5-dicarboxamide (3)**

Yield 51%; off-white solid; mp = 272–274 °C; <sup>1</sup>H NMR (400 MHz, DMSO-*d*<sub>6</sub>): δ 8.21 (t, *J* = 6.0 Hz, 1H), 8.07 (s, 1H), 7.71 (s, 1H), 7.34 (d, *J* = 8.8 Hz, 1H), 7.22 (t, *J* = 7.2 Hz, 1H), 7.09 (d, *J* = 6.4 Hz, 1H), 7.01 (d, *J* = 8.4 Hz, 1H), 6.83 (t, *J* = 7.6 Hz, 1H), 6.68 (s, 1H), 6.64 (dd, *J* = 2.0 Hz, *J* = 8.4 Hz, 1H), 6.19 (bs, 1H), 4.26 (d, *J* = 5.6 Hz, 2H), 3.748 (s, 2H), 3.74 (s, 3H), 2.55 (s, 3H); <sup>13</sup>C NMR (100 MHz, DMSO-*d*<sub>6</sub>): δ 170.56, 164.17, 163.18, 160.89, 157.09, 152.38, 149.65, 149.43, 147.19, 132.32, 128.50, 128.14, 127.07, 123.09, 120.43, 119.27, 111.26, 110.86, 93.12, 55.69, 47.71, 37.79, 14.39. MS (ESI) Calc. for [C<sub>23</sub>H<sub>22</sub>N<sub>6</sub>O<sub>5</sub>S + H]<sup>+</sup> = 495.14, found 495.05. HPLC showed 97.18% of purity.

**4.4.30. 4-Amino-N5-(2-((3,4-dichlorobenzyl)amino)-2-oxoethyl)-N5-(2-methylbenzo[d]oxazol-6-yl)isothiazole-3,5-dicarboxamide (4)**

Yield 39%; brown solid; mp = 265–267 °C; <sup>1</sup>H NMR (400 MHz, DMSO-*d*<sub>6</sub>): δ 8.55 (t, *J* = 5.6 Hz, 1H), 8.07 (s, 1H), 7.71 (s, 1H), 7.52 (d, *J* = 8.40 Hz, 1H), 7.39 (s, 1H), 7.34 (d, *J* = 8.0 Hz, 1H), 7.21 (dd, *J* = 1.60 Hz, *J* = 8.0 Hz, 1H), 6.62 (s, 1H), 6.60 (s, 1H), 6.25 (bs, 1H), 4.28 (d, *J* = 6.0 Hz, 2H), 3.74 (s, 2H), 2.51 (s, 3H); <sup>13</sup>C NMR (100 MHz, DMSO-*d*<sub>6</sub>): δ 170.52, 163.69, 162.70, 160.42, 151.88, 149.16, 148.94, 146.63, 140.85, 131.92, 130.81, 130.24, 129.15, 129.0, 127.54, 122.65, 118.82, 110.78, 92.56, 47.36, 40.96, 13.90. MS (ESI) Calc. for [C<sub>22</sub>H<sub>18</sub>Cl<sub>2</sub>N<sub>6</sub>O<sub>4</sub>S + H]<sup>+</sup> = 534.05, found 533.39. HPLC showed 95.72% of purity.

**4.4.31. 4-Amino-N5-(2-((4-methoxybenzyl)amino)-2-oxoethyl)-N5-(2-methylbenzo[d]oxazol-6-yl)isothiazole-3,5-dicarboxamide (5)**

Yield 58%; off-white solid; mp = 283–285 °C; <sup>1</sup>H NMR (400 MHz, DMSO-*d*<sub>6</sub>): δ 8.38 (t, *J* = 5.6 Hz, 1H), 8.08 (s, 1H), 7.72 (s, 1H), 7.33 (d, *J* = 8.40 Hz, 1H), 7.14 (d, *J* = 8.80 Hz, 2H), 6.83 (d, *J* = 8.80 Hz, 2H), 6.65 (d, *J* = 2.0 Hz, 1H), 6.62 (dd, *J* = 2.0 Hz, *J* = 8.80 Hz, 1H), 6.18 (bs, 1H), 4.22 (d, *J* = 6.0 Hz, 2H), 3.71 (s, 5H), 2.52 (s, 3H); <sup>13</sup>C NMR (100 MHz, DMSO-*d*<sub>6</sub>): δ 170.4, 164.17, 163.18, 160.87, 158.63, 152.37, 149.64, 149.43, 147.23, 132.30, 131.85, 129.01, 119.25, 114.04, 111.26, 93.11, 55.50, 47.77, 41.95, 14.38. MS (ESI) Calc. for [C<sub>23</sub>H<sub>22</sub>N<sub>6</sub>O<sub>5</sub>S + H]<sup>+</sup> = 495.52, found 495.05. HPLC showed 95.79% of purity.

**4.4.32. 4-Amino-N5-(2-((4-chlorobenzyl)amino)-2-oxoethyl)-N5-(2-methylbenzo[d]oxazol-6-yl)isothiazole-3,5-dicarboxamide (6)**

Yield 49%; brown solid; mp = 274–276 °C; <sup>1</sup>H NMR (400 MHz, DMSO-*d*<sub>6</sub>): δ 8.64 (t, *J* = 5.8 Hz, 1H), 7.93 (d, *J* = 2.0 Hz, 1H), 7.84–7.78 (m, 2H), 7.69–7.58 (m, 2H), 7.30–7.28 (m, 2H), 7.19–7.11 (m, 4H), 4.40 (d, *J* = 6.0 Hz, 2H), 3.73 (s, 2H), 2.52 (s, 3H); <sup>13</sup>C NMR (100 MHz, DMSO-*d*<sub>6</sub>): δ 167.86, 166.31, 163.75, 162.42, 151.21, 150.41, 146.70, 142.18, 136.98, 135.37, 129.15, 129.07, 129.69, 127.28, 122.11, 119.87, 115.0, 114.79, 113.60, 54.39, 41.87, 14.26. MS (ESI) Calc. for [C<sub>22</sub>H<sub>19</sub>ClN<sub>6</sub>O<sub>4</sub>S + H]<sup>+</sup> = 500.05, found 500.13. HPLC showed 96.8% of purity.

**4.4.33. 4-Amino-N5-(2-((4-bromobenzyl)amino)-2-oxoethyl)-N5-(2-methylbenzo[d]oxazol-6-yl)isothiazole-3,5-dicarboxamide (7)**

Yield 38%; pale yellow solid; mp = 286–288 °C; <sup>1</sup>H NMR (400 MHz, DMSO-*d*<sub>6</sub>): δ 8.52 (t, *J* = 5.6 Hz, 1H), 8.09 (s, 1H), 7.72 (s, 1H), 7.45 (d, *J* = 8.40 Hz, 2H), 7.34 (d, *J* = 8.40 Hz, 1H), 7.17 (d, *J* = 8.40 Hz, 2H), 6.64 (s, 1H), 6.62 (dd, *J* = 1.60 Hz, *J* = 8.80 Hz, 1H), 6.21 (bs, 1H), 4.26 (d, *J* = 6.0 Hz, 2H), 3.73 (s, 2H), 2.51 (s, 3H); <sup>13</sup>C NMR (100 MHz, DMSO-*d*<sub>6</sub>): δ 170.74, 164.17, 163.17, 160.91, 152.36, 149.65, 149.43, 147.19, 139.48, 132.35, 131.45, 129.91, 123.07, 120.15, 119.27, 111.25, 93.15, 47.81, 41.91, 14.39. MS (ESI) Calc. for [C<sub>22</sub>H<sub>19</sub>BrN<sub>6</sub>O<sub>4</sub>S + H]<sup>+</sup> = 544.04, found 545.43. HPLC showed 95.90% of purity.

**4.4.34. 4-Amino-N5-(2-methylbenzo[d]oxazol-6-yl)-N5-(2-oxo-2-((3-trifluoromethyl)benzyl)amino)ethyl)isothiazole-3,5-dicarboxamide (8)**

Yield 38%; white solid; mp = 271–273 °C; <sup>1</sup>H NMR (400 MHz, DMSO-*d*<sub>6</sub>): δ 8.68 (t, *J* = 5.6 Hz, 1H), 7.96 (d, *J* = 2.0 Hz, 1H), 7.82–7.76 (m, 2H), 7.69–7.58 (m, 2H), 7.30–7.28 (m, 2H), 7.19–7.11 (m, 4H), 4.39 (d, *J* = 6.0 Hz, 2H), 3.76 (s, 2H), 2.56 (s, 3H); <sup>13</sup>C NMR (100 MHz, DMSO-*d*<sub>6</sub>): δ 167.82, 166.39, 163.65, 162.47, 151.24, 150.41, 146.70, 142.18, 136.98, 135.37, 131.28, 130.64, 129.89, 128.34, 126.43, 124.25, 120.75, 115.41, 114.86, 113.71, 54.35, 41.86, 14.69. MS (ESI) Calc. for [C<sub>23</sub>H<sub>19</sub>F<sub>3</sub>N<sub>6</sub>O<sub>4</sub>S + H]<sup>+</sup> = 533.12, found 533.29. HPLC showed 95.9% of purity.

**4.4.35. 4-Amino-N5-(2-((2,5-dichlorobenzyl)amino)-2-oxoethyl)-N5-(2-methylbenzo[d]oxazol-6-yl)isothiazole-3,5-dicarboxamide (9)**

Yield 39%; brown solid; mp = 264–266 °C; <sup>1</sup>H NMR (400 MHz, DMSO-*d*<sub>6</sub>): δ 8.74 (t, *J* = 5.9 Hz, 1H), 7.89 (d, *J* = 2.0 Hz, 1H), 7.83–7.78 (m, 2H), 7.61–7.56 (m, 2H), 7.49 (s, 1H), 7.42 (s, 2H), 7.34 (d, *J* = 6.8 Hz, 1H), 7.24 (d, *J* = 7.1 Hz, 1H), 4.36 (d, *J* = 6.0 Hz, 2H), 3.71 (s, 2H), 2.52 (s, 3H); <sup>13</sup>C NMR (100 MHz, DMSO-*d*<sub>6</sub>): δ 167.79, 166.73, 163.42, 162.41, 151.91, 150.43, 146.50, 142.18, 136.98, 135.37, 129.15, 129.07, 126.82, 126.97, 122.11, 119.87, 116.0, 114.79, 114.60, 53.84, 41.89, 14.36. MS (ESI) Calc. for [C<sub>22</sub>H<sub>18</sub>Cl<sub>2</sub>N<sub>6</sub>O<sub>4</sub>S + H]<sup>+</sup> = 534.05, found 534.09. HPLC showed 96.1% of purity.

**4.4.36. 4-Amino-N5-(2-methylbenzo[d]oxazol-6-yl)-N5-(2-((3-methylbenzyl)amino)-2-oxoethyl)isothiazole-3,5-dicarboxamide (10)**

Yield 44%; white solid; mp = 264–266 °C; <sup>1</sup>H NMR (400 MHz, DMSO-*d*<sub>6</sub>): δ 8.54 (t, *J* = 5.8 Hz, 1H), 7.86 (d, *J* = 6.0 Hz, 1H), 7.81–7.75 (m, 2H), 7.69–7.58 (m, 2H), 7.30–7.28 (m, 2H), 7.19–7.11 (m, 4H), 4.29 (d, *J* = 6.0 Hz, 2H), 3.73 (s, 2H), 2.59 (s, 3H), 2.38 (s, 3H); <sup>13</sup>C NMR (100 MHz, DMSO-*d*<sub>6</sub>): δ 167.81, 166.49, 163.69, 162.46, 151.24, 150.41, 146.70, 142.18, 136.98, 131.34, 129.78, 129.22, 128.37, 126.43, 124.25, 120.75, 115.41, 114.86, 113.71, 54.35, 41.86, 23.8, 14.64. MS (ESI) Calc. for [C<sub>23</sub>H<sub>22</sub>N<sub>6</sub>O<sub>4</sub>S + H]<sup>+</sup> = 479.15, found 479.20. HPLC showed 97.3% of purity.

**4.4.37. 4-Amino-N5-(2-((3,5-dimethylbenzyl)amino)-2-oxoethyl)-N5-(2-methylbenzo[d]oxazol-6-yl)isothiazole-3,5-dicarboxamide (11)**

Yield 49%; brown solid; mp = 278–280 °C; <sup>1</sup>H NMR (400 MHz, DMSO-*d*<sub>6</sub>): δ 8.79 (t, *J* = 5.6 Hz, 1H), 7.84 (d, *J* = 2.0 Hz, 1H), 7.81–7.75 (m, 2H), 7.69–7.58 (m, 2H), 7.30 (s, 1H), 7.19–7.11 (m, 4H), 4.42 (d, *J* = 6.0 Hz, 2H), 3.74 (s, 2H), 2.36 (s, 6H); <sup>13</sup>C NMR (100 MHz, DMSO-*d*<sub>6</sub>): δ 167.83, 166.59, 164.02, 162.46, 151.24, 150.41, 146.70, 142.18, 136.98, 131.34, 129.78, 129.22, 128.37, 126.43, 124.25, 120.75, 115.41, 114.86, 113.71, 54.35, 41.86, 23.49, 14.58. MS (ESI) Calc. for [C<sub>24</sub>H<sub>24</sub>N<sub>6</sub>O<sub>4</sub>S + H]<sup>+</sup> = 493.16, found 493.31. HPLC showed 97.6% of purity.

**4.4.38. 4-Amino-N5-(2-((3-methyl-5-(trifluoromethoxy)benzyl)amino)-2-oxoethyl)-N5-(2-methylbenzo[d]oxazol-6-yl)isothiazole-3,5-dicarboxamide (12)**

Yield 31%; yellow solid; mp = 289–292 °C; <sup>1</sup>H NMR (400 MHz,

DMSO- $d_6$ ):  $\delta$  8.68 (t,  $J$  = 5.8 Hz, 1H), 7.92 (d,  $J$  = 2.0 Hz, 1H), 7.84–7.77 (m, 2H), 7.71–7.64 (m, 2H), 7.41 (s, 1H), 7.19–7.11 (m, 4H), 4.38 (d,  $J$  = 6.0 Hz, 2H), 3.76 (s, 2H), 2.56 (s, 3H), 2.39 (s, 3H);  $^{13}\text{C}$  NMR (100 MHz, DMSO- $d_6$ ):  $\delta$  167.83, 166.59, 164.02, 162.46, 162.23, 151.24, 150.41, 146.70, 142.18, 136.98, 134.18, 132.79, 130.28, 129.36, 127.41, 124.25, 121.81, 116.95, 114.26, 113.74, 54.39, 41.78, 23.38, 14.47. MS (ESI) Calc. for  $[\text{C}_{24}\text{H}_{21}\text{F}_3\text{N}_6\text{O}_5\text{S} + \text{H}]^+$  = 563.13, found 563.00.

#### 4.4.39. 4-Amino-N5-(2-((3-chloro-5-(trifluoromethyl)benzyl)amino)-2-oxoethyl)-N5-(2-methylbenzo[d]oxazol-6-yl)isothiazole-3,5-dicarboxamide (13)

Yield 30%; brown solid; mp = 287–289 °C;  $^1\text{H}$  NMR (400 MHz, DMSO- $d_6$ ):  $\delta$  8.92 (t,  $J$  = 5.9 Hz, 1H), 7.84 (d,  $J$  = 2.0 Hz, 1H), 7.84–7.77 (m, 2H), 7.71–7.64 (m, 2H), 7.41 (s, 1H), 7.19–7.11 (m, 4H), 4.39 (d,  $J$  = 6.0 Hz, 2H), 3.79 (s, 2H), 2.53 (s, 3H);  $^{13}\text{C}$  NMR (100 MHz, DMSO- $d_6$ ):  $\delta$  167.83, 166.59, 164.02, 162.46, 162.23, 151.24, 150.41, 146.70, 142.18, 136.98, 134.18, 132.79, 130.28, 129.36, 127.41, 124.22, 121.84, 116.35, 114.66, 113.69, 54.38, 41.82, 14.54. MS (ESI) Calc. for  $[\text{C}_{23}\text{H}_{18}\text{ClF}_3\text{N}_6\text{O}_4\text{S} + \text{H}]^+$  = 568.07, found 568.39. HPLC showed 95.2% of purity.

#### 4.4.40. 4-Amino-N5-(2-methylbenzo[d]oxazol-6-yl)-N5-(2-((2-methylbenzyl)amino)-2-oxoethyl)isothiazole-3,5-dicarboxamide (14)

Yield 51%, white solid; mp = 271–273 °C;  $^1\text{H}$  NMR (400 MHz, DMSO- $d_6$ ):  $\delta$  8.61 (t,  $J$  = 5.6 Hz, 1H), 7.93 (d,  $J$  = 2.0 Hz, 1H), 7.84–7.78 (m, 2H), 7.62–7.54 (m, 2H), 7.18–7.12 (m, 1H), 7.10–7.06 (m, 5H), 4.42 (d,  $J$  = 6.0 Hz, 2H), 3.74 (s, 2H), 2.54 (s, 3H), 2.28 (s, 3H);  $^{13}\text{C}$  NMR (100 MHz, DMSO- $d_6$ ):  $\delta$  167.72, 166.31, 163.75, 162.42, 159.6, 151.21, 150.41, 146.70, 142.18, 136.98, 135.37, 127.15, 126.82, 126.97, 122.11, 119.87, 115.0, 114.79, 113.20, 53.47, 52.71, 21.82, 14.27. MS (ESI) Calc. for  $[\text{C}_{23}\text{H}_{22}\text{N}_6\text{O}_4\text{S} + \text{H}]^+$  = 479.15, found 479.01. HPLC showed 96.7% of purity.

#### 4.4.41. 4-Amino-N5-(2-((3-chlorobenzyl)amino)-2-oxoethyl)-N5-(2-methylbenzo[d]oxazol-6-yl)isothiazole-3,5-dicarboxamide (15)

Yield 46%; pale yellow solid; mp = 261–263 °C;  $^1\text{H}$  NMR (400 MHz, DMSO- $d_6$ ):  $\delta$  8.48 (t,  $J$  = 5.2 Hz, 1H), 8.07 (s, 1H), 7.71 (s, 1H), 7.42 (d,  $J$  = 7.20 Hz, 1H), 7.35 (d,  $J$  = 8.40 Hz, 1H), 7.30–7.19 (m, 6H), 6.70 (s, 1H), 6.64 (dd,  $J$  = 2.0 Hz,  $J$  = 8.40 Hz, 1H), 6.23 (s, 1H), 4.36 (d,  $J$  = 6.0 Hz, 2H), 3.78 (s, 2H), 2.53 (s, 3H);  $^{13}\text{C}$  NMR (100 MHz, DMSO- $d_6$ ):  $\delta$  170.92, 164.17, 163.18, 160.93, 152.39, 149.64, 149.3, 147.19, 136.73, 132.41, 132.36, 129.51, 129.14, 129.02, 127.43, 123.14, 119.28, 111.27, 93.18, 47.70, 14.39. MS (ESI) Calc. for  $[\text{C}_{22}\text{H}_{19}\text{ClN}_6\text{O}_4\text{S} + \text{H}]^+$  = 500.8, found 499.26. HPLC showed 91.67% of purity.

### 4.5. DNA supercoiling assay

Supercoiling assay was performed using the commercially available *P. aeruginosa* DNA gyrase assay kit (Inspiralis Pvt. limited, Norwich, UK). The assay was performed in 1.5 mL eppendorf tubes at room temperature. 1 U of DNA gyrase was incubated with 0.5  $\mu\text{g}$  of relaxed pBR 322 DNA in 30  $\mu\text{L}$  reaction volume at 37 °C for 30 min [18] with 40 mM HEPES. KOH (pH 7.6), 10 mM magnesium acetate, 10 mM DTT, 2 mM ATP, 500 mM potassium glutamate, 0.05 mg/mL albumin (BSA). Standard compound novobiocin was the positive control and 4% DMSO was considered as negative control. Subsequently, each reaction was stopped by the addition of 30  $\mu\text{L}$  of stop dye [40% sucrose, 100 mM Tris-HCl (pH 7.5), 1 mM EDTA and 0.5 mg/mL bromophenol blue], briefly centrifuged for 45 s and supernatant was loaded and run in 1% agarose gel in 1X TAE buffer (40 mM Tris acetate, 2 mM EDTA). Furthermore, concentration of the range of compounds that inhibits 50% of supercoiling activity ( $\text{IC}_{50}$ ) was determined using densitometry and NIH image through Bio-Rad GelDoc image viewer.

### 4.6. *P. aeruginosa* susceptibility test

Pure colonies grown on agar are used to inoculate 3 mL of sterile broth to an OD of 0.6. One milliliter of this suspension is added to 29 mL of sterile water to provide the inoculum for the microdilution trays, which will be inoculated with a multipoint inoculator. Each test compound stock solutions will be diluted in nutrient broth by four-fold the final highest concentration to be tested. Compounds are diluted serially in a sterile 96-well microtiter plates using 100  $\mu\text{L}$  of nutrient broth. All the sampling will be done in duplicates. Plates will be incubated at 35 °C and readings are noted at 18 to 24 and 48 h. The MIC is considered as the lowest concentration of an antimicrobial agent that completely inhibited growth of the bacteria. Test carried out in the absence and presence of efflux pump inhibitor PA $\beta$ N (0.025 mg/mL) and conessine (0.02 mg/mL).

### 4.7. Molecular dynamics simulations

The Desmond module from Schrödinger was used for running MD simulations with periodic boundary conditions. The receptor & designed inhibitors complex was immersed in an orthorhombic simulation box, with the TIP3P explicit water model using the system builder panel with the minimum thickness of a solvent layer, 10 Å. In order to neutralize the system, counter ions were added.

Before equilibration and long production of MD simulations, the systems were minimized and pre-equilibrated using relaxation routine implemented in Desmond. Whereas, program ran six steps composed a) energy minimization was used by hybrid method of steepest descent and limited-memory Broyden-Fletcher-Goldfarb-Shanno (LBFSGS) algorithm with a maximum steps of 2000 including preliminary 10 steps of steepest descent with solute restrained, b) Energy minimization for 2000 steps without solute restraints, c) 12 ps simulation in NVT ensemble (temperature 10 K) restraining nonhydrogen solute atoms, d) 12 ps simulation in the NPT ensemble (temperature 10 K) restraining non-hydrogen solute atoms, e) 24 ps simulation in the NPT ensemble restrained along with solute non-hydrogen atoms (temperature 300 K) and f) 24 ps simulation in the NPT ensemble (temperature 300 K) with no restraints respectively. The temperatures and pressures in the short initial simulations were checked by applied Berendsen thermostats and barostats algorithms. The equilibrated system was simulated for 50 ns with a time step of 2 fs, NPT ensemble was used a Nosé-Hoover thermostat at 300 K and Martyna-Tobias-Klein barostat at 1.01325 pressure bar. A time step of 1.2 fs was used. Saving energy and structure enumerated for every 4.8 ps during simulation, the MD trajectory was generated. Finally to analyze trajectory simulation, a simulation interaction diagram tool was used.

### Declaration of Competing Interest

The authors declare that they have no known competing financial interests or personal relationships that could have appeared to influence the work reported in this paper.

### Acknowledgments

DS is thankful to Department of Biotechnology, Government of India for the Tata innovation fellowship (BT/HRD/35/01/04/2015). SJ is thankful to Albany Molecular Research center Hyderabad for providing financial support. VSK is thankful to Department of Science and Technology, Government of India for the INSPIRE fellowship (IF160108).

### Appendix A. Supplementary material

Supporting information files include spectral data ( $^1\text{H}$  and  $^{13}\text{C}$  NMR,

and MS) of the compounds. Supplementary data to this article can be found online at <https://doi.org/10.1016/j.bioorg.2020.103905>.

## References

- [1] J. Yayan, B. Ghebremedhin, K. Rasche, Antibiotic resistance of *Pseudomonas aeruginosa* in pneumonia at a single university hospital center in Germany over a 10-year period, *PLoS ONE* 10 (10) (2015) 0139836.
- [2] V.S. Ahirrao, A. Mauskar, T. Ravi, A study on common pathogens associated with nosocomial infections and their antibiotic sensitivity, *Int. J. Contemporary Pediatrics* 4 (2) (2017) 365–369.
- [3] M. Chatterjee, C.P. Anju, L. Biswas, V.A. Kumar, C.G. Mohan, R. Biswas, Antibiotic resistance in *Pseudomonas aeruginosa* and alternative therapeutic options, *Int. J. Med. Microbiol.* 306 (1) (2016) 48–58.
- [4] K. Botzenhart, G. Döring, Ecology and epidemiology of *Pseudomonas aeruginosa*, 1–18, *Pseudomonas aeruginosa* as an Opportunistic Pathogen, Springer, Boston, MA, 1993.
- [5] T. Strateva, D. Yordanov, *Pseudomonas aeruginosa* phenomenon of bacterial resistance, *J. Med. Microbiol.* 58 (9) (2009) 1133–1148.
- [6] D.E. Ehmman, S.D. Lahiri, Novel compounds targeting bacterial DNA topoisomerase/DNA gyrase, *Curr. Opin. Pharmacol.* 18 (2014) 76–83.
- [7] A. Kureishi, J.M. Diver, B. Beckthold, T. Schollaardt, L.E. Bryan, Cloning and nucleotide sequence of *Pseudomonas aeruginosa* DNA gyrase *gyrA* gene from strain PAO1 and quinolone-resistant clinical isolates, *Antimicrob. Agents Chemother.* 38 (9) (1994) 1944–1952.
- [8] V. Lamour, L. Hoermann, J.M. Jeltsch, P. Oudet, D. Moras, An open conformation of the thermophilus Gyrase B ATP-binding domain, *J. Biol. Chem.* 277 (21) (2002) 18947–18953.
- [9] S.C. Lovell, I.W. Davis, W.B. Arendall 3rd, P.I. De Bakker, J.M. Word, M.G. Prisant, J.S. Richardson, D.C. Richardson, Structure validation by calpha geometry: phi, psi and Cbeta deviation, *Proteins Struct. Funct. Bioinf.* 50 (3) (2003) 437–450.
- [10] M. Wiederstein, M.J. Sippl, ProSA-web: interactive web service for the recognition of errors in three-dimensional structures of proteins, *Nucleic Acids Res.* 35 (suppl\_2) (2007) W407–W410.
- [11] B. Wallner, A. Elofsson, Can correct protein models be identified, *Protein Sci.* 12 (5) (2003) 1073–1086.
- [12] W.L. DeLano, The PyMOL molecular graphics system, <http://www.pymol.org>, 2002.
- [13] V.S. Krishna, S. Zheng, E.M. Rekha, L.W. Guddat, D. Sriram, Discovery and evolution of novel mycobacterium tuberculosis ketol-acid reductoisomerase inhibitors and therapeutic drug leads, *J. Comput. Aided Mol. Des.* 33 (2019) 357–366.
- [14] R.A. Friesner, R.B. Murphy, M.P. Repasky, L.L. Frye, J.R. Greenwood, T.A. Halgren, P.C. Sanschagrin, D.T. Mainz, Extra precision glide: Docking and scoring incorporating a model of hydrophobic enclosure for protein–ligand complexes, *J. Med. Chem.* 49 (21) (2006) 6177–6196.
- [15] C.A. Lipinski, F. Lombardo, B.W. Dominy, P.J. Feeney, Experimental and computational approaches to estimate solubility and permeability in drug discovery and development settings, *Adv. Drug Deliv. Rev.* 23 (1–3) (1997) 3–25.
- [16] M. Abbraccio, I. Eberini, C. Parravicini, C. Martini, M.L. Trincavelli, S. Daniele, CENTRO CARDIOLOGICO MONZINO SpA, 2012. Gpr17-modulating compounds, diagnostic and therapeutic uses thereof, U.S. Patent Application 2012 14/556,007.
- [17] C. Jöst, C. Nitsche, T. Scholz, L. Roux, C.D. Klein, Promiscuity and selectivity in covalent enzyme inhibition: a systematic study of electrophilic fragments, *J. Med. Chem.* 57 (18) (2014) 7590–7599.
- [18] S.S. Walker, M. Labroli, R.E. Painter, J. Wiltsie, B. Sherborne, N. Murgolo, X. Sher, P. Mann, P. Zuck, C.G. Garlisi, J. Su, Antibacterial small molecules targeting the conserved TOPRIM domain of DNA gyrase, *PLoS ONE* 12 (7) (2017) e0180965.
- [19] B. Medapi, N. Meda, P. Kulkarni, P. Yogeewari, D. Sriram, Development of acridine derivatives as selective *Mycobacterium tuberculosis* DNA gyrase inhibitors, *Bioorg. Med. Chem.* 24 (4) (2016) 877–885.
- [20] L. Saiman, J.L. Burns, S. Whittier, J. Krzewinski, S.A. Marshall, R.N. Jones, Compliance of clinical microbiology Laboratories in the United States with current recommendations for Processing Respiratory Tract Specimens from Patients with Cystic Fibrosis, *J. Clin. Microbiol.* 37 (9) (1999) 2987–2991.
- [21] S.K. Tripathi, R. Muttineni, S.K. Singh, Targeting the cyclin-binding groove site to inhibit the catalytic activity of CDK2/cyclin A complex using p27<sup>KIP1</sup>-derived peptidomimetic inhibitors, *J. Theor. Biol.* 334 (2013) 87–100.
- [22] G.J. Martyna, D.J. Tobias, M.L. Klein, Constant pressure molecular dynamics algorithms, *J. Chem. Phys.* 101 (5) (1994) 4177–4189.